IEEE Access
Multidisciplinary ⋮ Rapid Review ⋮ Open Access Journal

Received January 21, 2021, accepted February 12, 2021, date of publication March 2, 2021, date of current version March 16, 2021.

Digital Object Identifier 10.1109/ACCESS.2021.3063192

Design of RBF Adaptive Sliding Mode Controller for A Supercavitating Vehicle

WANG JINGHUA[1,2], (Member, IEEE), LIU YANG[1], CAO GUOHUA[3], ZHAO YONGYONG[1], AND ZHANG JIAFENG[1]

[1]College of Mechanical and Electric Engineering, Changchun University of Science and Technology, Changchun 130022, China
[2]Ministry of Education Key Laboratory for Cross Scale Micro and Nano Manufacturing, Changchun University of Science and Technology, Changchun 130022, China
[3]Chongqing Research Institute, Changchun University of Science and Technology, Chongqing 401135, China

Corresponding author: Wang Jinghua (hit1920s@163.com)

This work was supported in part by the Defense Industrial Technology Development Program under Grant JCKY2019411B001, in part by the 111 Project of China under Grant D17017, in part by the Science and Technology Research Program of the Education Department of Jilin Province under Grant JJKH20181139KJ, in part by the Science and Technology Innovation Foundation of Changchun University of Science and Technology under Grant XJJLG-2017-13, and in part by the Innovation Foundation of Luquan under Grant LQ-2020-01.

ABSTRACT This paper proposes an adaptive sliding mode control strategy based on RBF (Radial Basis Function) neural network for the supercavitating vehicle system with model uncertainties and external disturbance. Aiming at the unknown items in the model, the control strategy compensates the unknown model uncertainty and external disturbance through the RBF neural network, and derives the neural network weight update strategy according to the Lyapunov stability theory which can guarantee the closed loop system asymptotic stability. The simulation results show that this control strategy can enable the supercavitating vehicle to track reference signal when there are model uncertainties and external disturbance, and ensure the convergence of the trajectory tracking error. Compared with the control input of the sliding mode control strategy without RBF neural network, the control input of the adaptive sliding mode control strategy with RBF neural network is also reduced, which further verifies the effectiveness of the RBF adaptive sliding mode control strategy proposed in this paper.

INDEX TERMS Adaptive sliding mode control, RBF neural network, supercavitating vehicle, supercavity.

I. INTRODUCTION

With the continuous development and utilization of marine resources by mankind, underwater unmanned vehicles have become an important carrier for exploring the ocean. The traditional underwater unmanned vehicle is completely wrapped by water, resulting in high resistance and low speed. At present, supercavitation technology has been used to develop a new generation of high-speed underwater vehicles [1]. When the underwater vehicle is sailing at a high enough speed, the fluid pressure drops below a specific value that cannot maintain a liquid state, and the entire area except the head and tail is wrapped by continuous bubbles, so that the vehicle surface does not come into direct contact with the liquid, thereby greatly reducing the viscous resistance of water [2], this kind of vehicle is called supercavitating vehicle. The supercavitating vehicle is surrounded by cavity envelope, which is different from the conventional hydrodynamic distribution, only the front cavitator and the fins are in direct contact with the liquid, so it is difficult to maintain stability during the voyage. It is precisely because of this characteristic of the supercavitating vehicle that its dynamic modeling and controller design have brought great challenges.

In recent years, there has been a lot of work about dynamic modeling of supercavitating vehicle. Kirschner *et al.* [3] proposed a nonlinear supercavitating vehicle dynamic model with 12 state variables and 6 degrees of freedom. A new type of supercavitating vehicle dynamics model was constructed based on experimental data, which simplified the nonlinear model to a nonlinear feedback LTI system with time delay and dead zone [4]. Dzielski and Kurdila [5] used the semiempirical steady state cavitation model to establish a simplified 2 degree of freedom classical longitudinal plane dynamic model under a fixed cavitation number. Wang and Liu [6] further studied the planing force of the fin based on

The associate editor coordinating the review of this manuscript and approving it for publication was Nasim Ullah.

the simplified model, and verified it through numerical calculations and experiments. Li *et al.* [7] considered the time delay effect of cavitation changes and conducted related experimental studies. Wei *et al.* [8] used the pole configuration method to control the cavitator angle of the supercavitating vehicle, the result shows that the stability of the supercavitating vehicle can be well maintained by controlling the rotation angle of the supercavitating vehicle. Zhou *et al.* [9] also considered the impact of angle of attack and other uncertain factors during the movement, and analyzed the uncertainty of the trajectory on this basis. Zhao *et al.* [10] established a mathematical model of a turning supercavitating vehicle and designed a complete state model, including a pitch channel and a yaw channel. He *et al.* [11] used the finite element method (FEM) to establish a two-way solid-liquid coupling program to obtain the fins load of the supercavitating vehicle. Wang *et al.* [12] and Mao and Wang [13] considered the time-varying fins efficiency, and the result shows that the dynamic equations established with consideration of the fins efficiency have higher practical value.

In a series of papers, the control strategies of supercavitating vehicle are studied. Dzielski and Kurdila [5] established a nonlinear model of supercavitating vehicle, and proposed a feedback linearization controller. Shao *et al.* [14] proposed a switching controller that can switch between two LQR controllers according to whether there is planing force. On the basis of Shao *et al.*, Vanek *et al.* [15] designed another feedback linearization switching controller, which switches when there is planing force. Lin and Balachandran [16] and Qiang [17] proposed a controller based on the circle criterion to achieve the absolute stability of the supercavitating vehicle. In order to deal with the catastrophic instability of supercavitating vehicles, Zhao *et al.* [18] proposed a dynamic flushing filter auxiliary feedback to control sudden changes. Robust control methods are mentioned in literature [4], [9], and the H-inf method and the LPV-H method are respectively proposed. Mao and Wang [13] designed a sliding mode controller, at the same time, they also proposed a linear parameter variable controller, and used an adaptive control method to explain the unknown planing force effectiveness parameter. Literature [20] proposed a fractional-order sliding mode controller, which uses fractional-order integral to calculate the non-integer integral or derivative in the sliding mode control algorithm, seeking better control for the control of supercavitating vehicles ability. An adaptive control law including adaptive fault-tolerant components is designed based on the inversion method [21]. The bounded adaptive law can estimate the upper limit of the unknown uncertainty, thereby ensuring that the supercavitating vehicle is in stability in case of failure.

Both the cavitation shape and the planing force formula are based on experimental results, in the face of the ever-changing external environment, the current technology cannot accurately calculate the true value, so the established dynamic model of the vehicle is uncertain. When the supercavitating vehicle is sailing at high-speed, turbulence and other phenomena will occur at the tail of the cavitation. The effects of these phenomena are difficult to express with specific equations, so it will bring unknown interference to the tail of the vehicle. An excellent controller should be able to adapt and compensate when faced with these unknown situations.

With the development of various fields of automation, the application of modern mathematics in system modeling and control is further promoted, which makes the control of uncertain systems easier. Among them, Li used the new numerical framework of Takagi-Sugeno (TS) – Tensor product Model Transformation (TPMT) to complete the modeling control design of the fuzzy system based on LMI [22]. In the absence of PMSG's ability to describe machine dynamics, a simplified impedance model of PMSG-WT is proposed to more accurately analyze the influence of MSM on system stability [23]. Authors in [24] fully considered the nonlinear of the DG system, developed the ET-PF filtering algorithm, and used the information in the previous event triggering strategy to enhance the estimated performance. Authors in [25] studied the vulnerability analysis and identification of key nodes of the power grid from the perspective of complex networks. The fusion of neural network and control algorithm further expands the research of uncertain systems. Among them, the radial basis function (RBF) neural network relies on its own powerful nonlinear mapping function, which can quickly approximate any nonlinear function, significantly improve the performance of the controller, and is particularly suitable for handling uncertain control problems [26]. For the unknown items of the biped robot, a control strategy based on the full state feedback and output feedback designed based on the RBF neural network is used, the result shows that the proposed control strategy can ensure the stability of the biped robot's attitude [27]. Aiming at the problem of robot trajectory tracking, an adaptive neural network switching control strategy was proposed to make the trajectory tracking error converge to zero in an infinite time [28]. For the tracking problem of uncertain link robots with full state constraints, adaptive neural network is used to deal with system uncertainty and disturbance, by selecting appropriate design parameters, the stability of the closed-loop system can be ensured [29]. Li *et al.* [30] proposed an adaptive RBF neural network control strategy based on global approximation for the trajectory tracking problem of supercavitating vehicle, and the network weights are designed and adjusted through the Lyapunov stability theory, so that the trajectory tracking error asymptotically converges to a small neighborhood of zero. Aiming at the uncertainty of the manipulator with elastic deformation, the RBF neural network is used to estimate and compensate the uncertainty of the system, and the stability of the system is proved by the Lyapunov stability theory [31].

This paper is mainly based on the RBF neural network to design an adaptive sliding mode control strategy. This control strategy is a nonlinear mapping composed of adaptive sliding mode control and RBF neural network. Its characteristic is that the neural network control is integrated into the adaptive

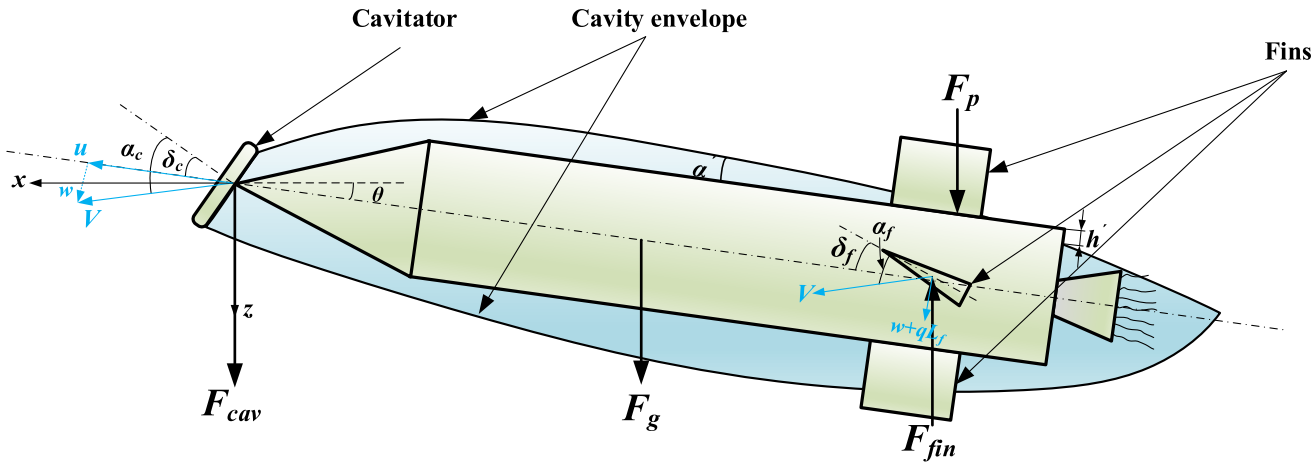

FIGURE 1. Structure diagram of supercavitating vehicle.

sliding mode control system, which enhances the robustness of the control system, and does not need to know the model uncertainty and external disturbance of the dynamic model in advance, but uses the RBF neural network to adapt learning model uncertainty and external disturbances. At the same time, the proposed control strategy can be updated online to compensate the unknown dynamic uncertainty of the system. The control system can ensure that under the condition of model uncertainty and external disturbance, the vehicle can track a reference signal and ensure the convergence of tracking errors. The structure of this paper is as follows: In the second part, the dynamic model of the supercavitating vehicle is derived. In the third part, designed an RBF neural network adaptive sliding mode controller, and gave the stability analysis proof. In the fourth part, simulation results are given to verify the effectiveness of the proposed RBF adaptive sliding mode controller. In the fifth part, give the conclusion.

II. DYNAMIC MODELING

When a supercavitating vehicle sails in the water, most of area of the vehicle is surrounded by cavity envelope, only the cavitator, fins and the tail of the vehicle are in contact with water, and the cavitator and fins provide lift and control force. When the tail of the vehicle hits the cavity envelope, a nonlinear planing force is generated. The structure of the supercavitating vehicle is shown in Fig.1, where the center of the cavitator O is the origin of the coordinate system, the x-axis points to the horizontal direction, the z-axis points to the earth, F_g is gravity and δ_c is the vertical line of the cavitator and the center line of the vehicle. F_{cav} is the control force generated by the cavitator, δ_f is the deflection angle of the fin relative to the centerline of the vehicle, F_{fin} is the lift generated by the fin, F_p is the nonlinear planing force, and α' is the angle between cavity envelope axis and the body, h' is the depth of the immersion of the body tail into the water.

A. EQUATION OF MOTION

According to the literature [5], the inertia matrix is

$$\begin{bmatrix} m & -mx_g \\ -mx_g & J \end{bmatrix} \tag{1}$$

where the mass of the vehicle $m = (7/9)k\rho\pi R^2 L$, moment of inertia $J = (11/60)k\rho\pi R^4 L + (133/405)k\rho\pi R^2 L^3$, center of mass coordinates $x_g = -(17/28)L$, the vehicle's length $L = 1.8m$, ρ is the density of water, k is the density ratio, R is the radius of the vehicle.

On the longitudinal plane, the attitude of the vehicle is represented by four parameters: depth z, pitch angle θ, vertical speed w and pitch rate speed q. The relationship between them is

$$\begin{cases} \dot{z} = w - V\theta \\ \dot{\theta} = q \end{cases} \tag{2}$$

where the travel speed $V = 75m/s$.

B. KINETIC MODEL

Because in the longitudinal plane, only the component force along the z-axis direction of the coordinate system plays a decisive role in the motion stability of the vehicle, so only the force in the z-axis direction needs to be considered in the dynamic equation. The state equation is

$$\begin{cases} F_{cav} + F_{fin} + F_g + F_p = m\dot{\omega} - mx_g\dot{q} - mVq \\ M_{fin} + M_g + M_p = -m\dot{\omega}x_g + J\dot{q} + mVx_g q \end{cases} \tag{3}$$

where the sum of the lift force in the longitudinal plane includes the force F_{cav} of the cavitator, the force F_{fin} of the fin, the gravity F_g and the planing force F_p. The pitch moment includes the fin moment M_{fin}, the gravity moment M_g and the planing force moment M_p.

The force of the cavitator is [5]

$$F_{cav} = C_x\alpha_c \tag{4}$$

where $C_x = 0.5c_{x0}(1+\sigma)\rho\pi R_n^2 V^2$, cavitation number $\sigma = 0.03$, drag coefficient $c_{x_0} = 0.82$. Since the origin of the body coordinate system is in the cavitator, the cavitator torque is zero. The relationship between the cavitator angle of attack α_c and the cavitator deflection angle δ_c is

$$\alpha_c = \tan^{-1}\left(\frac{w}{V}\right) + \delta_c \tag{5}$$

Since the fin is essentially equivalent to a wedge-shaped cavitator, the force of the elevator fin and the moment of fin can be known as [5]

$$\begin{cases} F_{fin} = -nC_x\alpha_f \\ M_{fin} = F_{fin}L \end{cases} \tag{6}$$

where the relationship between the fin angle of attack α_f and the fin deflection angle δ_f is

$$\alpha_f \approx \tan^{-1}\left(\frac{w+qL}{V}\right) + \delta_f \tag{7}$$

The component force of gravity in the z-axis direction of the body coordinate system is $F_g = mg\cos\theta$, and the moment M_g caused by gravity is

$$M_g = -mg\cos\theta x_g \tag{8}$$

It can be seen from the literature [5] that the planing force F_p generated by the fin of the vehicle against the cavity envelope is

$$\begin{cases} F_p = -\rho\pi R^2 V^2\left[1-\left(\frac{R'}{R'+h'}\right)^2\right]\left(\frac{1+h'}{1+2h'}\right)\alpha' \\ M_p = F_p L \end{cases} \tag{9}$$

$$h' = \begin{cases} 0 & |w| \le \frac{V(R_c-R)}{L} \\ \frac{L}{R}\left|\frac{w}{V}\right| - \frac{R_c-R}{R} & |w| > \frac{V(R_c-R)}{L} \end{cases}$$

$$\alpha' = \begin{cases} \frac{w-\dot{R}_c}{V} & w > 0 \\ \frac{w+\dot{R}_c}{V} & w \le 0 \end{cases} \tag{10}$$

where$R' = (R_c - R)/R$, R_c is the cavitator radius, R is the vehicle radius.

$$R_c = R_n\left(c_{x0}\frac{1+\sigma}{\sigma}\right)^{\frac{1}{2}}\kappa_2 \tag{11}$$

The rate of change of cavity radius $\dot{R}_c$ is

$$\dot{R}_c = \frac{-\frac{20}{17}\left(c_{x0}\frac{1+\sigma}{\sigma}\right)^{\frac{1}{2}} V\left(1-\frac{4.5\sigma}{1+\sigma}\right)\kappa_1^{\frac{23}{17}}}{\kappa_2\left(\frac{1.92}{\sigma}-3\right)} \tag{12}$$

$\kappa_1 = \frac{L}{R_n}\left(\frac{1.92}{\sigma}-3\right)^{-1} - 1$, $\kappa_2 = \left[1-\left(1-\frac{4.5\sigma}{1+\sigma}\right)\kappa_1^{\frac{40}{17}}\right]^{\frac{1}{2}}$. Where cavitator radius $R_n = 0.0191$m.

Bring all the forces and moments into Eq. (3), the final state equation is

$$\begin{aligned} \dot{x}(t) &= Ax(t) + Bu(t) + C_g + D_p F_p \\ &= \begin{bmatrix} 0 & -V & 1 & 0 \\ 0 & 0 & 0 & 1 \\ 0 & 0 & a_{33} & a_{34} \\ 0 & 0 & a_{43} & a_{44} \end{bmatrix} x(t) + \begin{bmatrix} 0 & 0 \\ 0 & 0 \\ b_{31} & b_{32} \\ b_{41} & b_{42} \end{bmatrix} u(t) \\ &\quad + \begin{bmatrix} 0 \\ 0 \\ g \\ 0 \end{bmatrix} + \begin{bmatrix} 0 \\ 0 \\ d_3 \\ d_4 \end{bmatrix} F_p \end{aligned} \tag{13}$$

where $x(t) = [z, \theta, w, q]^T$, $u(t) = [\delta_f, \delta_c]^T$ the parameters are as follows

$$\begin{aligned} a_{33} &= \frac{nCV}{k\left(aS-b^2\right)}\left[\frac{3}{4}b - \frac{S}{L}\right] \\ a_{34} &= \frac{nCV}{4k\left(aS-b^2\right)}\left[\frac{9}{4}bL - 3S\right] + V \\ a_{43} &= \frac{nCV}{k\left(aS-b^2\right)}\left[\frac{b}{L} - \frac{3}{4}a\right] \\ a_{44} &= \frac{nCV}{4k\left(aS-b^2\right)}\left[3b - \frac{9}{4}aL\right] \\ b_{31} &= \frac{nCV^2}{k\left(aS-b^2\right)}\left[\frac{3}{4}b - \frac{S}{L}\right] \\ b_{32} &= \frac{SCV^2}{k\left(aS-b^2\right)L} \\ b_{41} &= \frac{nCV^2}{k\left(aS-b^2\right)}\left[\frac{b}{L} - \frac{3}{4}a\right] \\ b_{42} &= \frac{-bCV^2}{k\left(aS-b^2\right)L} \\ d_3 &= \frac{S-bL}{k\rho\pi R^2 L\left(aS-b^2\right)} \quad d_4 = \frac{aL-b}{k\rho\pi R^2 L\left(aS-b^2\right)} \\ \tau_f &= \frac{L_f}{V}C = \frac{1}{2}c_x\frac{R_n^2}{R^2}c_x = c_{x0}(1+\sigma)c_{x0} = 0.82 \\ n &= 0.5 \quad a = \frac{7}{9} \quad b = \frac{17}{36}L \quad k = 2 \\ S &= \frac{11}{60}R^2 + \frac{133}{405}L^2 \end{aligned}$$

III. RBF NEURAL NETWORK ADAPTIVE SLIDING MODE CONTROL

This part proposes an adaptive sliding mode control strategy based on RBF neural network. The characteristic of this control strategy is that it is not necessary to know the model uncertainty and external disturbance of the supercavitating vehicle model, in addition, the powerful fitting ability of the RBF neural network is used for dynamic compensation of system uncertainties.

First, an adaptive sliding mode controller is designed for the kinetic model of a supercavitating vehicle with uncertainties. The sliding mode switching function $s(t) = 0$ is used to obtain the equivalent control u_{eq}, and the uncertainties in u_{eq} the term $E(x,t)$ is replaced by the unknown term γ and the sign function $\mathrm{sgn}(s)/||\mathrm{sgn}(s)||$, and then the switching control u_{vss} is obtained. The M_1 and M_2 in the u_{vss} are replaced with

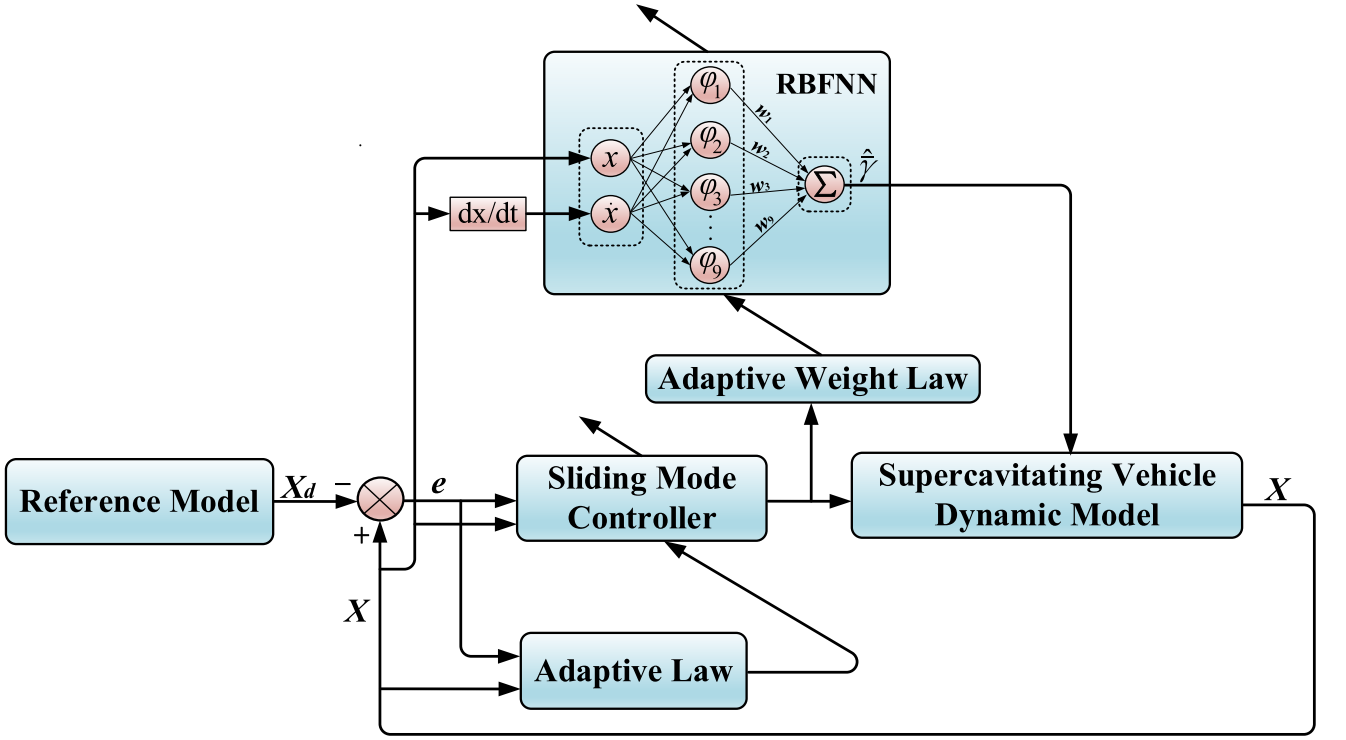

FIGURE 2. Flow chart of adaptive sliding mode control based on RBF neural network.

$\hat{M}_1(t)$ and $\hat{M}_2(t)$, the estimated value and the adaptive control law with the uncertainties term is obtained. The RBF neural network is used to estimate uncertain term $E(x,t)$, and the state variable $x(t)$ of the supercavitating vehicle is transmitted to the input of RBF neural network. By deriving the adaptive weights of the neural network through the Lyapunov stability theory, the uncertainty term $E(x,t)$ can be finally estimated.

By making a difference between the reference signal and the state variable of the supercavitating vehicle model, the error $e(t)$ is obtained which is regarded as the input of the sliding mode controller. Then the unknown item is estimated by use of the adaptive control law, RBF neural network, adaptive weights and etc. Finally, the closed-loop control system is showed in Fig.2.

A. PROBLEM DESCRIPTION AND ASSUMPTIONS

There is a big difference between a supercavitating vehicle and a conventional underwater vehicle. There are model uncertainties and external disturbance in supercavitating vehicle kinetic model. Uncertain changes in drag coefficient bring uncertainties to the kinetic model of the vehicle, the tail of vehicle will also be disturbed by unknown forces. It is impossible to have an accurate kinetic model, so it is necessary to design a suitable controller to compensate the uncertainties and disturbance.

According to the above analysis of uncertainties, considering the model uncertainties and external disturbance of the supercavitating vehicle, the vehicle kinetic model Eq. (13) is rewritten as the following nonlinear uncertainty system.

$$\dot{x}(t) = (A + \Delta A)x(t) + (B + \Delta B)u(t) + C_g + D_p F_p + f(t)$$

where ΔA represents the model uncertainty in matrix A, ΔB represents the model uncertainty in matrix B, $f\ (t)$ repersents the external disturbance received by the vehicle. For the convenience of the state equation processing, the model uncertainty ΔA, ΔB, external disturbance $f(t)$ are written together to become $E(x,t) = \Delta A x(t) + \Delta B u(t) + f(t)$.

Therefore, the modified state equation of supercavitating vehicle is

$$\dot{x}(t) = Ax(t) + Bu(t) + C_g + D_p F_p + E(x,t) \tag{14}$$

where $x(t) = [z, \theta, w, q]^T$, $u(t) = [\delta_f, \delta_c]^T$, $A \in R^{4\times4}$, $B \in R^{4\times2}$, $E(x,t) \in R^4$ is the system model's nonlinear uncertainty and external disturbance, the $E(x,t)$ is bounded.

The state equation of the reference signal is

$$\dot{x}_d(t) = A_d x_d(t) + B_d u_d(t) + C_g + D_p F_p \tag{15}$$

where $x_d(t) = [z_d, \theta_d, w_d, q_d]^T, u_d(t) \in R^2, A_d \in R^{4\times4}, B_d \in R^{4\times2}$ are derived from the reference signal.

Suppose the matrix $M_1 \in R^{4\times2}$ and the invertible matrix $M_2 \in R^{2\times2}$ satisfying

$$\begin{cases} A = A_d - BM_1^T \\ B = B_d M_2^{-1} \end{cases} \tag{16}$$

The task of control is to design a feedback control law $u(t)$ for the state equation, so that the state variable $x(t)$ asymptotically tracks the given reference signal $x_d(t)$.

B. ADAPTIVE SLIDING MODE CONTROLLER

The tracking error $e(t)$ is defined as

$$e(t) = x(t) - x_d(t) \tag{17}$$

The derivative of $e(t)$ with respect to time is

$$\begin{aligned}\dot{e}(t) &= Ax(t) + Bu(t) + E(x,t) - A_d x_d(t) - B_d u_d(t) \\ &= (A - A_d)x(t) + A_d e(t) + Bu(t) - B_d u_d(t) + E(x,t)\end{aligned} \tag{18}$$

The sliding mode switching surface $s(t)$ is defined as

$$s(t) = Ge(t) - GA_d \int_0^t e(\tau)d\tau \tag{19}$$

The sliding mode matrix $G \in R^{2\times 4}$.

$$\begin{aligned}\dot{s}(t) &= G\dot{e}(t) - GA_d e(t) \\ &= G(A - A_d)x(t) + GBu(t) - GB_d u_d(t) + GE(x,t)\end{aligned} \tag{20}$$

Let $\dot{s}(t) = 0$ get the equivalent control as

$$\begin{aligned}u_{eq}(t) &= (GB)^{-1}G(A_d - A)x(t) + (GB)^{-1}GB_d u_d(t) \\ &\quad -(GB)^{-1}GE(x,t) \\ &= M_1^T x(t) + M_2 u_d(t) - (GB)^{-1}GE(x,t)\end{aligned} \tag{21}$$

where $M_1^T = (GB)^{-1}G(A_d - A)$, $M_2 = (GB)^{-1}GB_d$.

Switch control u_{vss} is

$$u_{vss}(t) = M_1^T x(t) + M_2 u_d(t) - (GB)^{-1}G\gamma \frac{\mathrm{sgn}(s)}{\|\mathrm{sgn}(s)\|} \tag{22}$$

where γ is the model uncertainty and external disturbance.

According to Eq. (22), the adaptive control law u_{adp} is proposed is

$$u_{adp}(t) = \hat{M}_1^T(t)x(t) + \hat{M}_2(t)u_d(t) - (GB)^{-1}G\gamma \frac{\mathrm{sgn}(s)}{\|\mathrm{sgn}(s)\|} \tag{23}$$

$\hat{M}_1^T(t)$ and $\hat{M}_2(t)$ are the estimated values of M_1^T and M_2.

Define the parameters error $\tilde{M}_1^T(t)$ and $\tilde{M}_2(t)$ as

$$\begin{cases}\tilde{M}_1^T(t) = \hat{M}_1^T(t) - M_1^T \\ \tilde{M}_2(t) = \hat{M}_2(t) - M_2\end{cases} \tag{24}$$

Substitute Eq. (16), (23) and (24) into the system state equation Eq. (14)

$$\begin{aligned}\dot{x}(t) &= Ax(t) + B\left[\hat{M}_1^T(t)x(t) + \hat{M}_2(t)u_d(t)\right. \\ &\quad \left. -(GB)^{-1}G\gamma\frac{\mathrm{sgn}(s)}{\|\mathrm{sgn}(s)\|}\right] + E(x,t) \\ &= \left[A_d - BM_1^T\right]x(t) + B_d M_2^{-1}\left[\left(\tilde{M}_1^T(t) + M_1^T\right)x(t)\right. \\ &\quad \left. +\left(\tilde{M}_2(t) + M_2\right)u_d(t)\right] - B(GB)^{-1}G\gamma\frac{\mathrm{sgn}(s)}{\|\mathrm{sgn}(s)\|} \\ &\quad +E(x,t) \\ &= A_d x(t) + B_d\left[M_2^{-1}\tilde{M}_1^T(t)x(t) + M_2^{-1}\tilde{M}_2(t)u_d(t)\right] \\ &\quad +B_d u_d(t) - B(GB)^{-1}G\gamma\frac{\mathrm{sgn}(s)}{\|\mathrm{sgn}(s)\|} + E(x,t)\end{aligned} \tag{25}$$

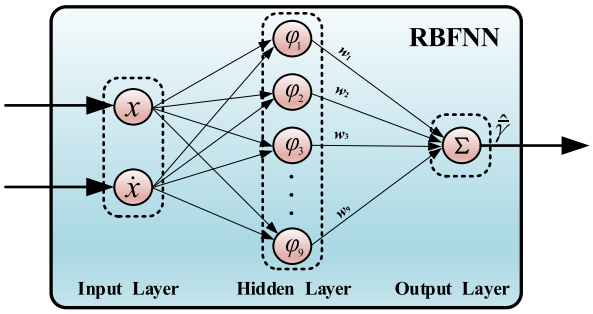

FIGURE 3. RBF neural network structure diagram.

Substitute Eq. (16), (23) and (24) into Eq. (18) to get

$$\begin{aligned}\dot{e}(t) &= (A - A_d)x(t) + A_d e(t) \\ &\quad +B_d\left[M_2^{-1}\tilde{M}_1^T(t)x(t) + M_2^{-1}\tilde{M}_2(t)u_d(t)\right] \\ &\quad +B_d M_2^{-1}M_1^T x(t) + B_d u_d(t) - B(GB)^{-1}G\gamma\frac{\mathrm{sgn}(s)}{\|\mathrm{sgn}(s)\|} \\ &\quad -B_d u_d(t) + E(x,t) \\ &= A_d e(t) + B_d\left[M_2^{-1}\tilde{M}_1^T(t)x(t) + M_2^{-1}\tilde{M}_2(t)u_d(t)\right] \\ &\quad -B(GB)^{-1}G\gamma\frac{\mathrm{sgn}(s)}{\|\mathrm{sgn}(s)\|} + E(x,t)\end{aligned} \tag{26}$$

Substitute Eq. (26) into Eq. (20) to get

$$\begin{aligned}\dot{s}(t) &= G\dot{e}(t) - GA_d e(t) \\ &= GB_d[M_2^{-1}\tilde{M}_1^T(t)x(t) + M_2^{-1}\tilde{M}_2(t)u_d(t)] \\ &\quad -G\gamma\frac{\mathrm{sgn}(s)}{\|\mathrm{sgn}(s)\|} + GE(x,t)\end{aligned} \tag{27}$$

C. RBF NEURAL NETWORK ADAPTIVE SLIDING MODE CONTROLLER

Suppose the upper limit of $\|E(x,t)\|$ is $\bar{\gamma}(x,t)$, the value of $\bar{\gamma}(x,t)$ is unknown, $\bar{\gamma}(x,t)$ can be obtained through the powerful approximation ability of the RBF neural network. The structure of RBF neural network consists of three layers, the structure is shown in Fig.3. The first layer is the input layer, the second layer is hidden layer and the third layer is output layer.

Where $x_1 = [z,\theta]^T, x_2 = \dot{x}_1 = [w,q]^T, x = [x_1,x_2]^T = [z,\theta,w,q]^T$, is the input of the RBF neural network, $\varphi_i(x)$ is the output value of the i-th hidden layer node.

The estimated value of $\hat{\bar{\gamma}}(x,t)$ is

$$\hat{\bar{\gamma}}(x,t) = \hat{w}^T\varphi(x) \tag{28}$$

where $\hat{w} \in R^9$ is the weight estimation vector, $\varphi(x) = [\varphi_1, \varphi_2, \ldots, \varphi_9]^T$, the radial phase basis function $\varphi_i(x)$ of each layer in the hidden layer selects the *Gauss* function

$$\varphi_i(x) = \exp\left(-\frac{\|x - c_i\|^2}{2\sigma_i^2}\right) \quad i = 1, 2, \ldots, 9 \tag{29}$$

$\varphi_i(x)$ is the output value of the i-th hidden layer node, c_i is the center vector of the i-th hidden layer, σ_i is the width of the i-th hidden layer, the center of the hidden layer c_i and the width σ_i iterative algorithm adopts literature [32]

$$\begin{cases} c_i(t) = c_i(t-1) + \eta\Delta c_i + \alpha\left[c_i(t-1) - c_i(t-2)\right] \\ \sigma_i(t) = \sigma_i(t-1) + \eta\Delta\sigma_i + \alpha\left[\sigma_i(t-1) - \sigma_i(t-2)\right] \end{cases} \tag{30}$$

where η is the learning rate, α is the momentum factor.

In order to compensate for external disturbance effectively, the best fit value of the RBF neural network is required to cover the upper limit of disturbance, the best weight $w*$ satisfies

$$w^{*T}\varphi(x) - \bar{\gamma}(x,t) = \varepsilon, 0 < \varepsilon < \varepsilon_1 \tag{31}$$

The upper limit of disturbance, $\bar{\gamma}(x,t)$, needs to be no less than external disturbance $E(x,t)$, so $\bar{\gamma}(x,t)$ and $E(x,t)$ satisfies

$$\bar{\gamma}(x,t) - \|E(x,t)\| \geq \varepsilon_0, \varepsilon_0 > \varepsilon_1 \tag{32}$$

Define the Lyapunov function

$$V = \frac{1}{2}\left\{s^T s + tr\left[\tilde{M}_1\Gamma^{-1}\tilde{M}_1^T\right] + tr\left[\tilde{M}_2\Gamma^{-1}\tilde{M}_2^T\right] + \xi^{-1}\|G\|\tilde{w}^T\tilde{w}\right\} \tag{33}$$

$\tilde{w} = w^* - \hat{w}, \xi = \varepsilon_0 - \varepsilon_1, \Gamma = M_2 Q = \Gamma^T > 0$, Γ is a positive definite matrix.

The derivation of the Lyapunov function is

$$\begin{aligned} \dot{V} &= s^T\dot{s} + tr\left[\tilde{M}_1\Gamma^{-1}\dot{\tilde{M}}_1^T\right] + tr\left[\tilde{M}_2\Gamma^{-1}\dot{\tilde{M}}_2^T\right] \\ &\quad -\xi^{-1}\|G\|\tilde{w}^T\dot{\hat{w}} \\ &= s^T\left\{GB_d\left[M_2^{-1}\tilde{M}_1^T(t)x(t) + M_2^{-1}\tilde{M}_2(t)u_d(t)\right]\right. \\ &\quad \left. +GE(t) - G\gamma\frac{\mathrm{sgn}(s)}{\|\mathrm{sgn}(s)\|}\right\} \\ &\quad +tr\left[\tilde{M}_1\Gamma^{-1}\dot{\tilde{M}}_1^T\right] + tr\left[\tilde{M}_2\Gamma^{-1}\dot{\tilde{M}}_2^T\right] - \xi^{-1}\|G\|\tilde{w}^T\dot{\hat{w}} \\ &= s^T\left[GF(t) - G\gamma\frac{\mathrm{sgn}(s)}{\|\mathrm{sgn}(s)\|}\right] + \left\{s^T GB_d M_2^{-1}\tilde{M}_1^T(t)x(t)\right. \\ &\quad \left. +tr\left[\tilde{M}_1\Gamma^{-1}\dot{\tilde{M}}_1^T\right]\right\} \\ &\quad + \left\{s^T GB_d M_2^{-1}\tilde{M}_2(t)u_d(t) + tr\left[\tilde{M}_2\Gamma^{-1}\dot{\tilde{M}}_2^T\right]\right\} \\ &\quad -\xi^{-1}\|G\|\tilde{w}^T\dot{\hat{w}} \end{aligned} \tag{34}$$

Let Eq. (34) $\begin{cases} s^T GB_d M_2^{-1}\tilde{M}_1^T(t)x(t) + tr\left[\tilde{M}_1\Gamma^{-1}\dot{\tilde{M}}_1^T\right] = 0 \\ s^T GB_d M_2^{-1}\tilde{M}_2(t)u_d(t) + tr\left[\tilde{M}_2\Gamma^{-1}\dot{\tilde{M}}_2^T\right] = 0 \end{cases}$,

to get the control law parameters $\dot{\tilde{M}}_1^T(t)$, $\dot{\tilde{M}}_2(t)$ and $\dot{\tilde{M}}_1^T(t)$, $\dot{\tilde{M}}_2(t)$

$$\begin{cases} \dot{\tilde{M}}_1^T(t) = \dot{\hat{M}}_1^T(t) = -Q^T B_d^T G^T s x^T \\ \dot{\tilde{M}}_2(t) = \dot{\hat{M}}_2(t) = -Q^T B_d^T G^T s u_d^T \end{cases} \tag{35}$$

Substitute Eq. (31), (32) and (35) into Eq. (34) to get

$$\begin{aligned} \dot{V} &= s^T\left[GF(x,t) - G\gamma\frac{\mathrm{sgn}(s)}{\|\mathrm{sgn}(s)\|}\right] - \xi^{-1}\|G\|\tilde{w}^T\dot{\hat{w}} \\ &\leq \|s\|\left[\|G\|\cdot\|E(x,t)\| - \|G\|\cdot\gamma\cdot\left\|\frac{\mathrm{sgn}(s)}{\|\mathrm{sgn}(s)\|}\right\|\right] \\ &\quad -\xi^{-1}\|G\|\tilde{w}^T\dot{\hat{w}} \\ &= \|s\|\left[\|G\|\cdot\|E(x,t)\| - \|G\|\cdot\gamma + \|G\|\cdot\bar{\gamma} - \|G\|\cdot\bar{\gamma}\right] \\ &\quad -\xi^{-1}\|G\|\tilde{w}^T\dot{\hat{w}} \\ &= -\|s\|\cdot\|G\|\left(\bar{\gamma} - \|E(x,t)\|\right) \\ &\quad +\|s\|\cdot\|G\|\left(\bar{\gamma} - \gamma\right) - \xi^{-1}\|G\|\tilde{w}^T\dot{\hat{w}} \\ &= -\|s\|\cdot\|G\|\left(\bar{\gamma} - \|E(x,t)\|\right) \\ &\quad +\|s\|\cdot\|G\|\left[w^{*T}\varphi(x) - \varepsilon - \hat{w}^T\varphi(x)\right] - \xi^{-1}\|G\|\tilde{w}^T\dot{\hat{w}} \\ &= -\|s\|\cdot\|G\|\left(\bar{\gamma} - \|E(x,t)\|\right) - \|s\|\cdot\|G\|\varepsilon \\ &\quad +\|G\|\left[\|s\|\tilde{w}^T\varphi(x) - \xi^{-1}\tilde{w}^T\dot{\hat{w}}\right] \end{aligned} \tag{36}$$

Adaptive weight is

$$\dot{\hat{w}} = \xi\|s\|\varphi(x) \tag{37}$$

Substitute Eq. (31), (32) and (37) into Eq. (36) to get

$$\begin{aligned} \dot{V} &= -\|s\|\cdot\|G\|\left(\bar{\gamma} - \|E(x,t)\|\right) - \|s\|\cdot\|G\|\cdot\varepsilon \\ &\leq -\|s\|\cdot\|G\|\left(\bar{\gamma} - \|E(x,t)\|\right) + \|s\|\cdot\|G\|\cdot\varepsilon \\ &\leq -\|s\|\cdot\|G\|\cdot\varepsilon_0 + \|s\|\cdot\|G\|\cdot|\varepsilon| \\ &\leq -\|s\|\cdot\|G\|\cdot\varepsilon_0 + \|s\|\cdot\|G\|\cdot\varepsilon_1 \\ &= -\|s\|\cdot\|G\|\left(\varepsilon_0 - \varepsilon_1\right) \leq 0 \end{aligned} \tag{38}$$

Therefore, the Lyapunov stability theory proves that the system has asymptotic stability. From the inequality (38), $s(t)$ can be integrated as $-\int_0^t\|s(\tau)\|d\tau \leq [V(t) - V(0)]/[\|G\|(\varepsilon_0 - \varepsilon_1)]$, when $V(0)$ and $V(t)$ are both bounded, $\lim_{t\to\infty}\int_0^t\|s(\tau)\|d\tau$ is also bounded, from Barbalat's lemma $\lim_{t\to\infty}s(t) \to 0$, therefore, it can be known from the sliding mode switching surface $s(t)$, $\lim_{t\to\infty}e(t) \to 0$.

IV. SIMULATION ANALYSIS

In order to verify the effectiveness of the proposed RBF neural network adaptive sliding mode control strategy, this part uses the RBF neural network adaptive sliding mode control strategy to simulate the kinetic model with model uncertainty and external disturbance of the supercavitating vehicle. The trajectory tracking performance, tracking error, response of each state variable and planing force are obtained through simulation, and the results show that the control strategy using RBF neural network to compensate for model uncertainty and external disturbance has achieved excellent tracking performance. Finally, by comparing the control input with and without the uncertainty estimated by the RBF neural

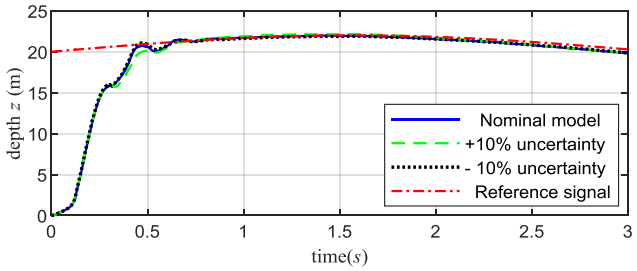

FIGURE 4. Supercavitating vehicle actual depth.

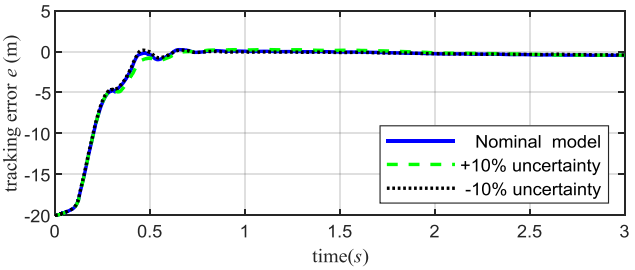

FIGURE 5. Supercavitating vehicle tracking error.

network, the effectiveness of the proposed control strategy is illustrated.

By the proposed control strategy to control the kinetic model of the supercavitating vehicle. At a depth of 0m, the supercavitating vehicle tracks a reference signal $z_d(t) = 2\sin(t) + 20$ with a depth of 20m and an amplitude of 2m with the initial state $x(0) = [0, 0, 2, 0]^T$, the state equation of the reference signal can be obtained by calculation

$$\dot{x}_d(t) = \begin{bmatrix} 0 & 0 & 1 & 0 \\ 0 & 0 & 0 & 0 \\ -1 & 0 & 0 & 0 \\ 0 & 0 & 0 & 0 \end{bmatrix} x_d(t) + \begin{bmatrix} 0 & 0 \\ 0 & 0 \\ 1 & 0 \\ 0 & 0 \end{bmatrix} \begin{bmatrix} 20 \\ 0 \end{bmatrix}$$

The sliding mode matrix G of the sliding mode surface is selected as

$$G = \begin{bmatrix} 5.5 & -75 & 1 & 0 \\ 0 & 4 & 0 & 1 \end{bmatrix}$$

The selected RBF neural network structure is 4-9-1. The initial weight ω is arbitrary, the initial hidden layer width $\sigma = 5$, the initial hidden layer center c is

$$c = \begin{bmatrix} -4 & -3 & -2 & -1 & 0 & 1 & 2 & 3 & 4 \\ -4 & -3 & -2 & -1 & 0 & 1 & 2 & 3 & 4 \\ -4 & -3 & -2 & -1 & 0 & 1 & 2 & 3 & 4 \\ -4 & -3 & -2 & -1 & 0 & 1 & 2 & 3 & 4 \end{bmatrix}$$

The hidden layer width σ and center c are iteratively updated according to Eq. (30).

Model uncertainty is mainly caused by changes in drag coefficient. In order to verify the effectiveness of the proposed RBF neural network adaptive sliding mode control strategy against model uncertainty and external disturbance, drag coefficient is changed by $\pm 10\%$, the external disturbance takes 10% of the planing force, $\Delta c_{x0} = \pm 10\% c_{x0}$, $||f(t)|| = 10\% F_p$.

The simulation results are shown in Fig.4 and Fig.5. It can be seen from Fig.4 and Fig.5 that the supercavitating vehicle can dive into a predetermined depth of 20m in about 0.5s. It can be seen from Fig.4 that in about 1s the applying $\pm 10\%$ uncertainty model and the nominal model can track the reference signal. It can be seen from Fig.5 that applying $\pm 10\%$ uncertainty model and the nominal model tracking error drops rapidly in the first 0.5s, and finally converges to zero. Therefore, it can be concluded that by using the RBF neural network adaptive sliding mode control strategy,

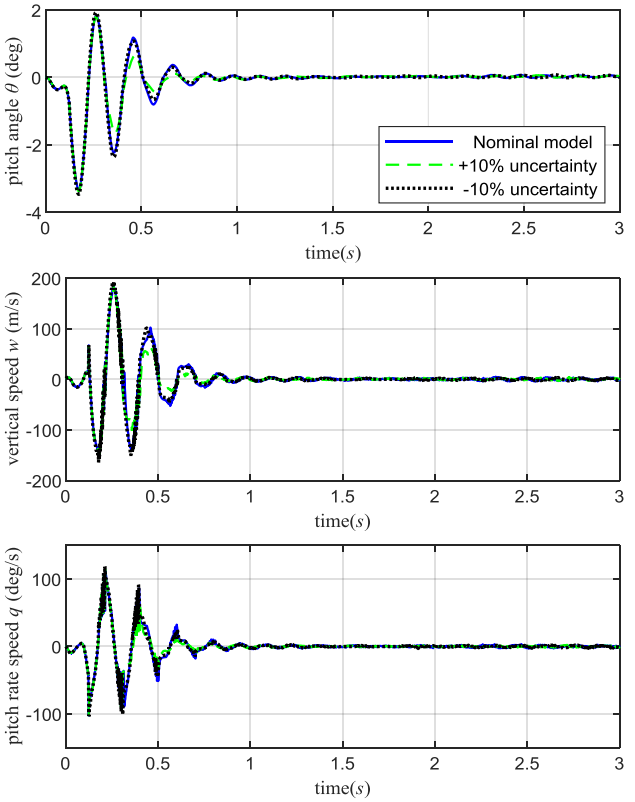

FIGURE 6. Pitch angle θ, vertical speed w and pitch rate speed q status response.

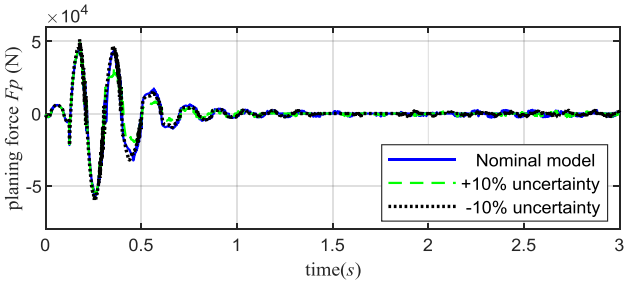

FIGURE 7. Planing force.

the supercavitating vehicle can track the reference signal under the condition of model uncertainty and external disturbance.

It can be seen from Fig.6 and Fig.7 that the curves of pitch angle θ, vertical speed w, pitch rate speed q and planing

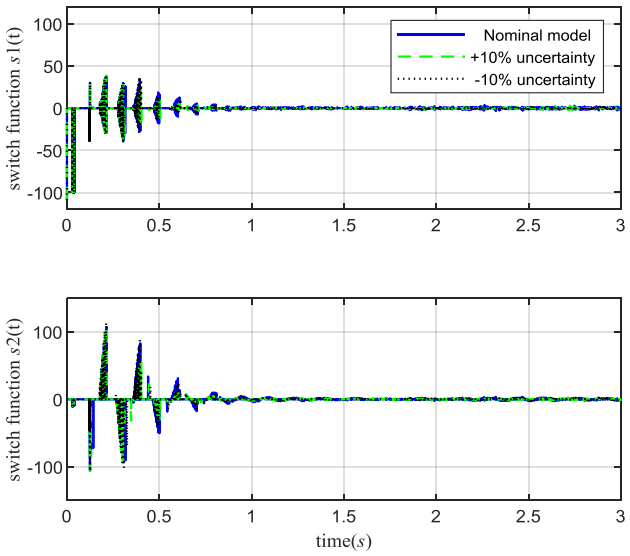

FIGURE 8. Switch function.

force F_p almost coincide, indicating that the supercavitating vehicle can control its status well in the face of $\pm 10\%$ uncertainty. θ, w, q and F_p have all undergone major changes in the first 1s, the reason is that the initial stage of sailing is in the rapid dive stage, which caused a drastic change in the state. In the subsequent stages, the response of each state tends to be generally stable, the reason for the small oscillation is that the trajectory of the vehicle tracking is a nonlinear sinusoidal curve, the navigation state of the vehicle needs to be adjusted at any time, which causes the various state quantities and planing forces to follow, small fluctuations in the stage.

It can be seen from Fig.8 that the switching functions $s_1(t)$ and $s_2(t)$ of the state variables z and θ have changed drastically in the initial stage, the reason is that the supercavitating vehicle is in rapid decline at this time. In the latent phase, there is a big difference between the actual state and the predetermined state. The subsequent switching function $s_1(t)$ almost approaches zero, indicating that the vehicle has tracked the predetermined trajectory; the switching function $s_2(t)$ still oscillates slightly, because the deflection angle of the vehicle needs to adjust at any time when tracking the nonlinear trajectory. The adjustment in a small range causes the switching function $s_2(t)$ to oscillate in a small range, but the oscillation amplitude is within a controllable range.

The result of using RBF neural network to compensate the $\pm 10\%$ uncertainty model and nominal model is shown in Fig. 9. The RBF neural network is used to adjust the gain of the switch part of the adaptive sliding mode control input. Fig.10 is the control input with the uncertainty estimated by the RBF neural network, Fig.11 is the control input without the RBF neural network. Comparing Fig.10 and Fig.11, it can see that the control input of the former is better, because whether it is during the dive stage at 0∼1s or the stable tracking stage afterwards, at the same moment, the control input amplitude in Fig.10 both are smaller than those in Fig.11,

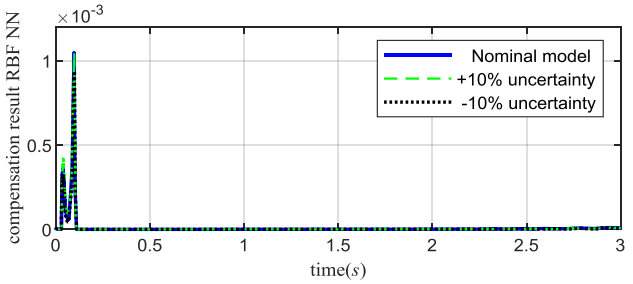

FIGURE 9. The result of using RBF neural network to compensate model uncertainty and external distrubance.

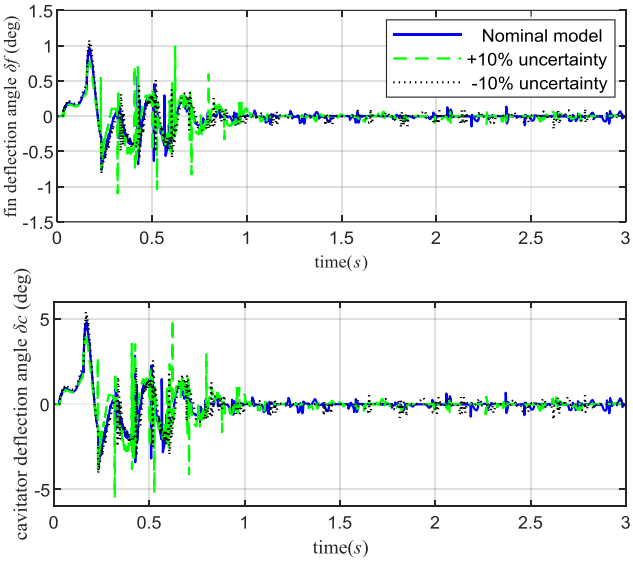

FIGURE 10. The control input with the uncertainty estimated by the RBF neural network.

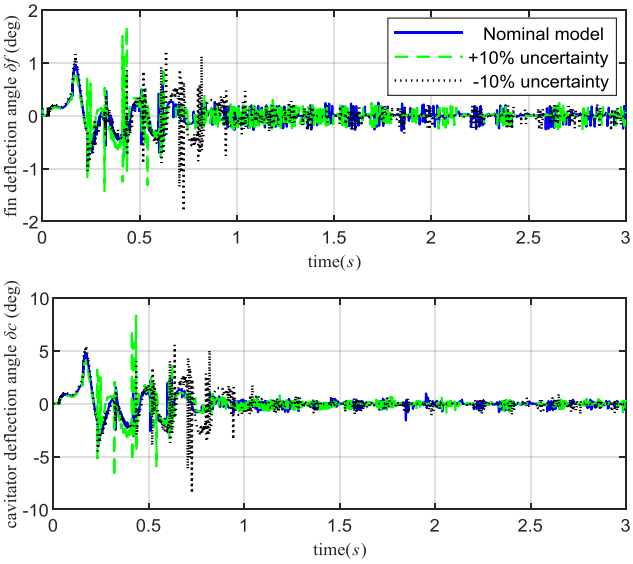

FIGURE 11. The control input without the RBF neural network.

that is at this moment the deflection angle of the fin and the cavitator are smaller. In the same time, a smaller deflection amplitude can reduce the difficulty of designing the control

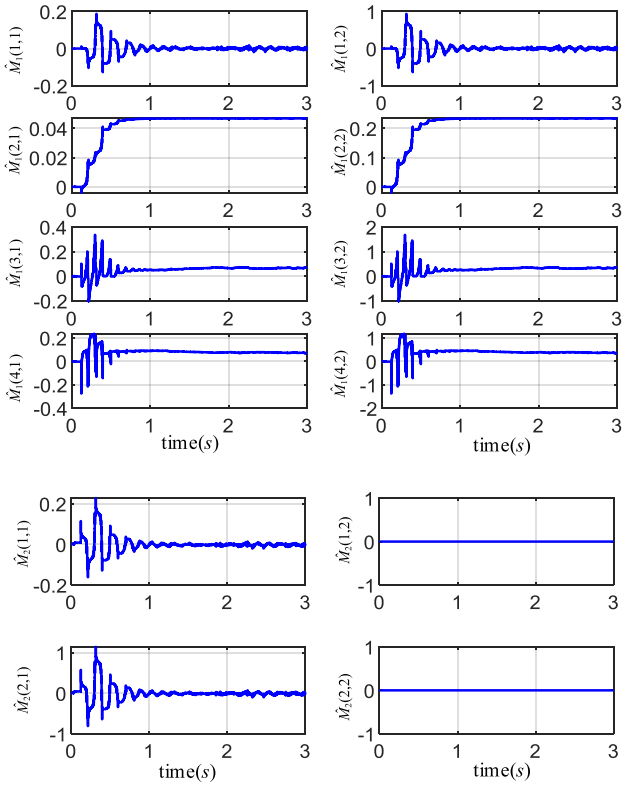

FIGURE 12. Time-varying estimation parameter $\hat{M}_1(t)$ and $\hat{M}_2(t)$ in adaptive control law.

mechanism and greatly reduce the load on the deflection mechanism.

Fig.12 is the parameter estimation matrix and values in the adaptive control strategy proposed in Eq. (23). The various variables in the matrix changed drastically in the early stage because the supercavitating vehicle was diving rapidly and its navigation attitude changed drastically. In the later stage, when the vehicle tracks the reference signal, the various parameters gradually stabilized. Although there are small changes in individual parameters, the reason for small-scale changes is that the control matrix of the controller needs to be adjusted in real time when faced with model uncertainty and external disturbances.

Therefore, it can be concluded that the dynamic system response of the supercavitating vehicle in line with expectations. The simulation results show that under the adaptive sliding mode control strategy based on RBF neural network, the supercavitating vehicle has excellent tracking performance, the tracking error asymptotically converges to zero. The proposed intelligent control strategy can compensate the model uncertainty and external disturbance of the supercavitating vehicle model, and make the system more robust.

V. CONCLUSION

This paper proposes an adaptive sliding mode control strategy based on RBF neural network for supercavitating vehicle model. This control strategy can be obtained through the powerful fitting ability of the RBF neural network without knowing the model uncertainty and the external disturbance from the outside. This control strategy can be obtained through the powerful fitting ability of the RBF neural network without knowing the model uncertainty and external disturbance of the kinetic model. The output of RBF neural network is used as uncertainty compensation parameter, which can eliminate the influence of model uncertainty and unknown external disturbance. The stability of the proposed RBF neural network adaptive sliding mode control strategy is proved by Lyapunov theory. The effectiveness and convergence of the proposed RBF neural network adaptive sliding mode control strategy are verified by simulation. The simulation results show that the tracking error almost asymptotically converge to 0.

REFERENCES

[1] S. Ashley, "Warp drive underwater," *Sci. Amer.*, vol. 284, no. 5, pp. 70–79, May 2001. [Online]. Available: https://www.jstor.org/stable/26059211

[2] Y. Zhang, X. Yuan, and F. Deng, *Fluid Dynamic of Supercavitating Underwater Vehicles*, 1st ed. Beijing, China: National Defense Industry Press, 2014.

[3] I. N. Kirschner, D. C. Kring, A. W. Stokes, N. E. Fine, and J. S. Uhlman, "Control Strategies For Supercavitating Vehicles," *J. Vibrat. Control*, vol. 8, pp. 219–242, Feb. 2002, doi: 10.1177/.107754602023818.

[4] E. S. David, J. B. Gary, and E. A. A. Roger, "Planing avoidance control for supercavitating vehicles," in *Proc. Amer. Control Conf. (ACC)*, Portland, OR, USA, 2014, pp. 4979–4984, doi: 10.1109/ACC.2014.6859485.

[5] J. Dzielski and A. Kurdila, "A benchmark control problem for supercavitating vehicles and an initial investigation of solutions," *J. Vibrat. Control*, vol. 9, no. 7, pp. 791–804, Jul. 2003, doi: 10.1177/1077546303009007004.

[6] W. Zou and H. Liu, "Modeling and simulations of the supercavitating vehicle with its tail-slaps," *J. Fluids Eng.*, vol. 137, no. 4, pp. 557–560, Apr. 2015, doi: 10.1115/1.4029330.

[7] D. Li, K. Luo, C. Huang, J. Dang, and Y. Zhang, "Dynamics model and control of high-speed supercavitating vehicles incorporated with time-delay," *Int. J. Nonlinear Sci. Numer. Simul.*, vol. 15, nos. 3–4, pp. 221–230, Jan. 2014, doi: 10.1515/ijnsns-2013-0063.

[8] P. Wei, J. Hou, and T. F. Chen, "Analysis on the stability of supercavitation projectile," *Appl. Mech. Mater.*, vols. 157–158, pp. 58–61, Feb. 2012, doi: 10.4028/www.scientific.net/AMM.157-158.58.

[9] L. Zhou, Y. Li, Z. Xue, J. Han, and N. Zhang, "Rigid-flexible-cavity coupling trajectory and uncertainty trajectory analysis of supercavitating projectiles," *Ocean Eng.*, vol. 126, pp. 138–151, Nov. 2016, doi: 10.1016/j.oceaneng.2016.08.032.

[10] X.-H. Zhao, Y. Sun, G.-L. Zhao, and J.-L. Fan, "μ-synthesis robust controller design for the supercavitating vehicle based on the BTT strategy," *Ocean Eng.*, vol. 88, pp. 280–288, Sep. 2014, doi: 10.1016/j.oceaneng.2014.06.035.

[11] Q. He, Y. Wei, C. Wang, and J. Zhang, "Imapct dynamics of supercavitating projectile with fluid/structure interaction," *Harbin Inst. Technol*, vol. 20, pp. 101–106, Feb. 2013, doi: 1005-9113(2013)01-0101-06.

[12] J. Wang, K. Yu, Y. Wei, C. Wang, and R. Lv, "Accelerated motion control of a supercavitating vehicle," in *Proc. 3rd Int. Symp. Syst. Control Aeronaut. Astronaut.*, Jun. 2010, pp. 1271–1275, doi: 10.1109/ISSCAA.2010.5633154.

[13] X. Mao and Q. Wang, "Adaptive control design for a supercavitating vehicle model based on fin force parameter estimation," *J. Vibrat. Control*, vol. 21, pp. 1220–1233, Apr. 2015, doi: 10.1177/.1077546313496263.

[14] Y. Shao, M. Mesbahi, and G. Balas, "Planing, switching, and supercavitating flight control," in *Proc. AIAA Guid., Navigat., Control Conf. Exhib.*, Aug. 2003, p. 5724, doi: 10.2514/6.2003-5724.

[15] B. Vanek, J. Bokor, G. J. Balas, and R. E. A. Arndt, "Longitudinal motion control of a high-speed supercavitation vehicle," *J. Vibrat. Control*, vol. 13, no. 2, pp. 159–184, Feb. 2007, doi: 10.1177/1077546307070226.

[16] G. Lin, B. Balachandran, and E. H. Abed, "Dynamics and control of supercavitating vehicles," *J. Dyn. Syst., Meas., Control*, vol. 130, no. 2, pp. 281–287, Mar. 2008, doi: 10.1115/1.2837307.

[17] B. Qiang, Y. Sun, Y. Han, and T. Bai, "Absolute stability control of supercavitating vehicles based on backstepping," in *Proc. IEEE Int. Conf. Mechatronics Autom.*, Aug. 2014, pp. 1918–1923.

[18] X. Zhao, Y. Sun, Z. Qi, and M. Han, "Catastrophe characteristics and control of pitching supercavitating vehicles at fixed depths," *Ocean Eng.*, vol. 112, pp. 185–194, Jan. 2016, doi: 10.1016/j.oceaneng.2015.12.021.

[19] X. Zhang, Y. Han, T. Bai, Y. Wei, and K. Ma, "H_∞ controller design using LMIs for high-speed underwater vehicles in presence of uncertainties and disturbances," *Ocean Eng.*, vol. 104, pp. 359–369, Aug. 2015, doi: 10.1016/j.oceaneng.2015.05.026.

[20] B. D. H. Phuc, V.-D. Phung, S.-S. You, and T. D. Do, "Fractional-order sliding mode control synthesis of supercavitating underwater vehicles," *J. Vibrat. Control*, vol. 26, nos. 21–22, pp. 1909–1919, Nov. 2020, doi: 10.1177/1077546320908412.

[21] Y. Bai, J. D. Biggs, Z. Zhang, and Y. Ding, "Adaptive fault-tolerant control for longitudinal motion of supercavitating vehicles," *Eur. J. Control*, vol. 57, pp. 263–272, Jan. 2021, doi: 10.1016/j.ejcon.2020.06.002.

[22] Y. Yu, Z. Li, X. Liu, K. Hirota, X. Chen, T. Fernando, and H. H. C. Iu, "A nested tensor product model transformation," *IEEE Trans. Fuzzy Syst.*, vol. 27, no. 1, pp. 1–15, Jan. 2019, doi: 10.1109/tfuzz.2018.2851575.

[23] B. Liu, Z. Li, X. Dong, S. S. Yu, X. Chen, A. M. T. Oo, X. Lian, Z. Shan, and X. Liu, "Impedance modeling and controllers shaping effect analysis of PMSG wind turbines," *IEEE J. Emerg. Sel. Topics Power Electron.*, early access, Aug. 5, 2021, doi: 10.1109/jestpe.2020.3014412.

[24] B. Liu, Z. Li, X. Chen, Y. Huang, and X. Liu, "Recognition and vulnerability analysis of key nodes in power grid based on complex network centrality," *IEEE Trans. Circuits Syst. II, Exp. Briefs*, vol. 65, no. 3, pp. 346–350, Mar. 2018, doi: 10.1109/TCSII.2017.2705482.

[25] X. Liu, L. Li, Z. Li, X. Chen, T. Fernando, H. H. C. Iu, and G. He, "Event-trigger particle filter for smart grids with limited communication bandwidth infrastructure," *IEEE Trans. Smart Grid*, vol. 9, no. 6, pp. 6918–6928, Nov. 2017, doi: 10.1109/TSG.2017.2728687.

[26] T. Chen and H. Chen, "Approximation capability to functions of several variables, nonlinear functionals, and operators by radial basis function neural networks," *IEEE Trans. Neural Netw.*, vol. 6, no. 4, pp. 904–910, Jul. 1995, doi: 10.1109/72.392252.

[27] C. Sun, W. He, W. Ge, and C. Chang, "Adaptive neural network control of biped robots," *IEEE Trans. Syst., Man, Cybern. Syst.*, vol. 47, no. 2, pp. 315–326, Feb. 2017, doi: 10.1109/TSMC.2016.2557223.

[28] L. Yu, S. Fei, L. Sun, and J. Huang, "An adaptive neural network switching control approach of robotic manipulators for trajectory tracking," *Int. J. Comput. Math.*, vol. 91, no. 5, pp. 983–995, Sep. 2013, doi: 10.1080/00207160.2013.813021.

[29] W. He, Y. Chen, and Z. Yin, "Adaptive neural network control of an uncertain robot with fullstate constraints," *IEEE Trans. Cybern.*, vol. 46, pp. 620–629, Mar. 2016, doi: 10.1109/TCYB.2015.2411285.

[30] Y. Li, M. Liu, X. Zhang, and X. Peng, "Global approximation based adaptive RBF neural network control for supercavitating vehicles," *J. Syst. Eng. Electron.*, vol. 29, no. 4, pp. 797–804, Dec. 2018, doi: CNKI:.SUN:XTGJ.0.2018-04-015.

[31] M. Ölgün and U. Tilki, "Neural network based sliding mode controller with genetic algorithm for two link robot manipulator," *Eur. J. Ence Theology*, pp. 120–129, 2020, doi: 10.31590/ejosat.araconf16.

[32] M. Wei and G. Chen, "Adaptive RBF neural network sliding mode control for ship course control system," in *Proc. 3rd Int. Conf. Intell. Hum.-Mach. Syst. Cybern.*, Aug. 2011, pp. 27–30, doi: 10.1109/IHMSC.2011.77.

WANG JINGHUA (Member, IEEE) received the Ph.D. degree from the Harbin Institute of Technology, in 2010. He is currently a Lecturer with the College of Mechanical and Electric Engineering, Changchun University of Science and Technology. His research interests include mobile robots, unmanned systems, and intelligent control.

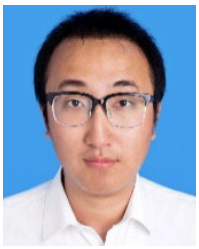

LIU YANG received the bachelor's degree in mechatronic engineering from the Shenyang University of Technology. He is currently pursuing the master's degree in engineering with the College of Mechanical and Electric Engineering, Changchun University of Science and Technology. His research interests include intelligent control and under water vehicle.

CAO GUOHUA received the bachelor's degree from Yanshan University, in 1988, and the master's and Ph.D. degrees from the Changchun University of Science and Technology, in 1991 and 2009, respectively. He is currently a Professor with the Chongqing Research Institute, Changchun University of Science and Technology. He is named as Special allowance of the State Council, State Class Persons of National Talents Engineering of Ministry of Personnel, and New Century Excellent Talents in Universities, Ministry of Education, China. His research interest includes electromechanical system control theory and technology.

ZHAO YONGYONG received the B.S. degree in instrument science and technology from the Xi'an University of Technology. He is currently pursuing the Ph.D. degree in mechanical engineering with the Changchun University of Science and Technology. His research interests include intelligent control, basic research on the gait of multi-legged robots, and probabilistic robots.

ZHANG JIAFENG is currently pursuing the master's degree with the Changchun University of Science and Technology. His research interests include advanced motor control algorithms and supercavitating vehicle control.